1 ***Daphnia magna* modifies its gene expression extensively in**

2 **response to caloric restriction revealing a novel effect on**

3 **haemoglobin isoform preference**

4

5 Jack Hearn[*1], Jessica Clark[2], Philip J. Wilson[3], and Tom J. Little[4]

6

7 [1]Department of Vector Biology, Liverpool School of Tropical Medicine, Liverpool,

8 United Kingdom

9 [2]Institute of Biodiversity, Animal Health & Comparative Medicine, University of

10 Glasgow, United Kingdom

11 [3]School of Geosciences, University of Edinburgh, Edinburgh, United Kingdom

12 [4]Institute of Evolutionary Biology, School of Biological Sciences, University of

13 Edinburgh, Edinburgh, United Kingdom

14 [*]corresponding author: Jack.Hearn@lstmed.ac.uk

15 **Email addresses:**

16 JH: Jack.Hearn@lstmed.ac.uk

17 JC: jessica.clark@glasgow.ac.uk

18
19 PJW: phil.wilson@ed.ac.uk

20 TJL: Tom.Little@ed.ac.uk

21

26   **Abstract**

27

28   Caloric restriction (CR) produces clear phenotypic effects within and between

29   generations of the model crustacean *Daphnia magna*. We have previously

30   established that micro RNAs and cytosine methylation change in response to CR in

31   this organism, and we demonstrate here that CR has a dramatic effect on gene

32   expression. Over 6000 genes were differentially expressed between CR and well-fed

33   *D. magna*, with a bias towards up-regulation of genes under caloric restriction. We

34   identified a highly expressed haemoglobin gene that responds to CR by changing

35   isoform proportions. Specifically, a transcript containing three erythrocruorin domains

36   was strongly down-regulated under CR in favour of transcripts containing fewer or no

37   such domains. This change in the haemoglobin mix is similar to the response to

38   hypoxia in *Daphnia,* which is mediated through the transcription factor hypoxia-

39   inducible factor 1, and ultimately the mTOR signalling pathway. This is the first report

40   of a role for haemoglobin in the response to CR. We also observed high absolute

41   expression of super-oxide dismutase (SOD) in normally-fed individuals, which

42   contrasts with observations of high SOD levels under in CR in other taxa. However,

43   key differentially expressed genes, like SOD, were not targeted by differentially

44   expressed micro-RNAs. Whether the link between Haemoglobin and CR is the case

45   in other organisms, or is related to the aquatic lifestyle, remains to be tested. It

46   suggests that one response to CR may be to simply transport less oxygen and lower

47   respiration.

48

49

50

51

Introduction

53

54 Caloric restriction (CR) is the reduction in dietary intake of calories without

55 undernutrition (Koubova & Guarente, 2003). CR induces marked phenotypic

56 changes in many organisms. Most notably an increase in longevity has been

57 observed in various arthropods, rodents, yeast, and possibly also humans (Heilbronn

58 & Ravussin, 2003; Kapahi, Kaeberlein, & Hansen, 2017; Lakowski & Hekimi, 1998;

59 Redman & Ravussin, 2011; Sohal & Weindruch, 1996; Walford, Harris, & Weindruch,

60 1987). This occurs through CR-mediated delays in the onset of processes and

61 diseases associated with ageing (Koubova & Guarente, 2003; Most, Tosti, Redman,

62 & Fontana, 2017). As a result, moderate CR could well be beneficial to human

63 health, although this remains to be confirmed by sufficiently long-running clinical

64 trials (Most et al., 2017).

65

66 The transcriptomic response to CR has been investigated in a variety of model

67 organisms spanning mammals, invertebrates and yeasts (Choi et al., 2018; Ding et

68 al., 2014; Dobson et al., 2018; Heintz et al., 2017; Kapahi et al., 2017; Kim et al.,

69 2016; Matthews et al., 2017; Regan et al., 2016; Wood et al., 2015). Neuroprotective

70 qualities of CR have been attributed to an altered gene expression profile of CR rats

71 due to an altered response to oxidative stress and histone deacetlyase activity, in

72 addition to changes to insulin-signalling pathway and longevity-associated gene

73 levels (Wood et al., 2015). In *Drosophila* CR responses have been characterised at

74 the whole-organism and tissue-level (Ding et al., 2014; Dobson et al., 2018; Kapahi

75 et al., 2017; Regan et al., 2016). There is an overall down-regulation of genes under

76 CR (Ding et al., 2014), which is a hallmark of CR (Russell & Kahn, 2007). However,

77 despite the popularity of *Daphnia magna* for studying life-history traits and the effects

78 of environmental stressors (Boersma, Spaak, & De Meester, 1998; Garbutt & Little,

79 2014, 2017; Lampert, 1987; Latta IV, Frederick, & Pfrender, 2011; Mitchell &

80 Lampert, 2000; Orsini et al., 2016), the gene-level response to CR has not previously

81 been studied in this species.

82

83 **Environmental stressors and caloric restriction in *Daphnia magna***

84

85 There is a wealth of existing phenotypic data in *Daphnia*, including demonstrations of

86 CR-mediated lifespan increase (Latta IV et al., 2011), which we confirm and expand

87 upon here. There are also clear maternal effects due to CR where *D. magna*

88 mothers exposed to CR produce offspring that are (1) larger at birth, (2) feed at a

89 slower rate than offspring of abundantly fed mothers, and are (3) more resistant to

90 parasitism (Garbutt & Little, 2014, 2017). Furthermore, *Daphnia* are aquatic

91 invertebrates, and it is possible that they respond to CR in a manner that is partially

92 distinct from terrestrial invertebrates. We explore this novel perspective in the

93 context of haemoglobins here.

94

95 ***Daphnia* Haemoglobins and the link to CR**

96

97 Haemoglobin (henceforward "Hb") production was observed to increase in response

98 to food levels in *D. magna* (Fox, Gilchrist, & Phear, 1951; Zeis, 2020). However, no

99 further studies considered the relationship between nutrition and Hb in *Daphnia*. By

100 contrast, it is well established that the response to hypoxia and hyper-thermal stress

101 in *D. magna* and *D. pulex* causes changes in Hb concentration and subunit

102 components to occur (Cuenca Cambronero, Zeis, & Orsini, 2018; Gerke, Börding,

103 Zeis, & Paul, 2011; Lai et al., 2016; Lyu et al., 2015; Zeis et al., 2003). This suggests

104 that there is phenotypic plasticity in the *Daphnia* Hb response to stress. Interestingly,

105 acclimation to hypoxic conditions in *D. magna* results in smaller adults without

106 impacting on clutch size during the first five broods (Seidl, Paul, & Pirow, 2005). A

107 phenotype which is similar to that for the offspring of CR individuals (Garbutt & Little,

108 2014). Links between nutrition and hypoxia have not been explored widely, but in

109 *Drosophila* a specifically low-protein CR regime partially reverses the reduction in

110 lifespan caused by hypoxia (Vigne & Frelin, 2006).

111

112 *Daphnia magna* encodes 12 di-domain Hb genes [as annotated in the gene-set:

113 (Orsini et al., 2016)] that result from a complex series of duplications (Colbourne et

114 al., 2011; Zeis, 2020). Sixteen Hb di-domains are aggregated to form the free-

115 circulating *D. magna* Hb molecule (Zeis, 2020). Structural differences in Hb

116 molecules comprised of the products of different Hb isoforms is correlated to

117 changes in oxygen-binding characteristics (Zeis, 2020). The induction of Hb genes in

118 *Daphnia* is mediated by the transcription factor hypoxia-inducible factor (HIF) (Gorr,

119 Cahn, Yamagata, & Bunn, 2004; Zeis, 2020), a heterodimer formed from HIF-1α and

120 HIF-1β proteins. The HIF-1 complex is an important factor in extending longevity of

121 *Caenorhabditis elegans* under CR (Di Chen & Kapahi, 2009; Lee, Hwang, & Kenyon,

122 2010; Y. Zhang, Shao, Zhai, Shen, & Powell-Coffman, 2009). Increased expression

123 of HIF-1 alone was responsible for this and was triggered by elevated concentrations

124 of mitochondrial reactive oxygen species (Lee et al., 2010). HIF-1 itself is regulated

125 by the mTOR pathway (Land & Tee, 2007) and in *C. elegans* is dependent on the

126   inosotol-requiring protein-1 (IRE-1) of the unfolded protein stress response in the

127   endoplasmic reticulum (Di Chen & Kapahi, 2009; Kapahi et al., 2017).

128

129   **Master control mechanisms underpinning CR responses**

130

131   The free radical theory of ageing has been linked to CR (Gladyshev, 2014; Liochev,

132   2013; Viña, Borras, Abdelaziz, Garcia-Valles, & Gomez-Cabrera, 2013). The theory

133   hypothesises that ageing results from accumulated oxidative damage due to reactive

134   oxygen species. Super-oxide dismutase (SOD), a key component of the theory

135   (Gladyshev, 2014), defends against reactive oxygen species (ROS) by converting

136   abundant superoxide into hydrogen peroxide and oxygen. Evidence that lacking

137   SOD genes results in reduced lifespans across taxa supports this hypothesis (Muid,

138   Karakaya, & Koc, 2014; Muller et al., 2006; Oka, Hirai, Yasukawa, Nakahara, &

139   Inoue, 2015).

140

141   Four nutrient-sensing, signalling pathways are most often implicated in lifespan

142   extension as a result of CR (Kenyon, 2010). They are 1) the insulin/insulin-like

143   growth factor (IGF-1), 2) the mechanistic target of rapamycin (mTOR) signalling

144   pathway, 3) 5' adenosine monophosphate-activated protein kinase (AMP Kinase),

145   and 4) sirtuin signalling protein-modulated pathways. These pathways are complex

146   and interlinking, with mTOR signalling potentially acting as the ultimate modulator of

147   the other three (Johnson, Rabinovitch, & Kaeberlein, 2013).

148

149   **The present study adds expression data to data on *D. magna* miRNA and DNA**

150   **methylation responses to CR**

151

152   To characterise phenotypic and genotypic ageing in a single organism, we

153   performed a whole organism longevity experiment on a set of eight *D. magna*

154   genotypes each subjected to a calorically restricted and normal diet. To contrast

155   gene expression between food levels, we selected one genotype that demonstrated

156   increased longevity here. We have previously established that life history traits

157   (Garbutt & Little, 2014, 2017), DNA methylation (Hearn, Pearson, Blaxter, Wilson, &

158   Little, 2019), and miRNA expression in the selected strain (Hearn et al., 2018)

159   respond to CR; indeed the miRNA was sequenced from the same set of RNA

160   extractions. Using gene and transcript level expression change of this CR-

161   responsive genotype of *D. magna* we now identify known and novel gene families

162   and metabolic pathways implicated in CR.

163

164   **Materials and Methods**

165

166   **Longevity experiment**

167

168   This experiment used eight genotypes from geographically dispersed populations.

169   These were obtained from the *D. magna* diversity panel held in Basel, Switzerland

170   (http://evolution.unibas.ch/ebert/research/referencepanel/).   They   are   (clone   ID,

171   Country of Origin): BEK22 (Belgium), Clone 32 (UK), FIFAV1 (Finland), GBEL75

172   (UK), GG8 (Germany), ILPS1 (Italy), MNDM1 (Mongolia), RUYAK1-6 (Russia). Prior

173   to the experiments, replicates of all genotypes were put through three generations of

174   acclimation to harmonise environmental effects arising from variation in stock

175   conditions. During this period, each individual was maintained in a 60ml glass jar

176   filled with artificial pond medium (Kluttgen et al., 1994). This was changed twice

177   weekly and when offspring were produced. Each individual was fed ~6.25 x 10^6

178   *Chlorella vulgaris* cells daily and was maintained on a 12:12 L:D cycle at 20ºC. We

179   estimate cell numbers by measuring the daily optical absorbance of 650nm white

180   light by the *Chlorella* culture, with 1.0 absorbance being equivalent to approximately

181   5 × 10^6 algal cells. Offspring from the second clutch initiated each generation,

182   including the experimental generation.

183   From the acclimated females of all eight genotypes, two offspring from clutch two

184   were taken. One was assigned to normal food (NF: ~6.25 x 10^6 cells as per

185   acclimation) and one was assigned to a caloric restriction (CR: ~1.4 x 10^6 cells)

186   treatment, which is approximately 20% of the amount of food available to NF

187   replicates. Each food treatment and genotype combination were replicated 24 times.

188   Date of birth and date of death were recorded. They were otherwise maintained

189   identically to the acclimation period.

190   **Survival Analysis**

191   A Cox's proportional hazards model was used to test for differences in longevity

192   between the two food treatments for all eight genotypes. This was done using the

193   survival package in R (code used and model outputs: Supplementary File S1, clone

194   longevity input data: Supplementary File S2). The response variable was days alive,

195   with genotype, food treatment and their interaction (days alive = clone + food +

196   clone*food), as fixed effects. There was no censoring as all individuals were followed

197   from their day of birth to the day of death. We present the results of the analysis of

198   deviance (ANOVA) for the Cox's model which performs $\chi2$-tests of likelihood ratios

199   of each model factor sequentially, which in this case was food followed by clone

200   followed by the interaction between them.

201   **Material for RNA harvesting**

202

203   Clone 32 (UK) (Auld, Hall, Housley Ochs, Sebastian, & Duffy, 2014) was selected for

204   RNA sequencing because it showed a longevity response in the above experiment,

205   and it shows clear maternal effects under variation in maternal food - larger offspring

206   are produced under CR (Garbutt & Little, 2014, 2017). This clone was also the focus

207   of more detailed analysis of food and longevity (Clark, Wilson, McNally and Little, *In*

208   *revision*) where it again showed lifespan extension in response to food restriction. To

209   generate RNA, maternal lines of C32 were first acclimatized for three generations in

210   artificial pond medium at 20°C and on a 12h:12h light:dark cycle and fed 2.5 x 10^6

211   cells of the single-celled green algae *Chlorella vulgaris* daily. The treatment

212   generation [G_0 in (Hearn et al., 2018)] was then split into two groups of eight

213   replicates paired by mother and fed either a normal diet of 5 x 10^6 algal cells/day or a

214   caloric restricted diet of 1 x 10^6 algal cells/day per individual. Each replicate was

215   formed of five *D. magna* reared in the same jar from birth.

216

217   After the birth of the first clutch of offspring in a replicate jar, the jar was treated for

218   microbial contamination with tetracycline and ampicillin (as described in Hearn et al.,

219   2018) over 24 hours, then *D. magna* individuals were homogenised in 700ul Qiazol

220   Qiagen reagent ID: 79306), and stored at -70°C until further processed. RNA was

221   extracted using miRNeasy mini kits (Qiagen Cat No./ID: 74106) and integrity and

222   quality checked by Qubit (Thermo Fisher) fluorometer, nanodrop (Thermo Fisher)

223   and Bioanalyzer (Agilent). No degradation was observed on Bioanalyzer total RNA

224 traces. Extractions were subsequently halved and one half was used to create small

225 RNA libraries for miRNA expression analysed in (Hearn et al., 2018). TruSeq

226 stranded mRNA-seq (Illumina, San Diego, USA) libraries were prepared by

227 Edinburgh Genomics from the remaining RNA for eight normal food and caloric-

228 restricted replicates as for the previous study. All libraries were multiplexed and

229 sequenced on one lane of HiSeq 4000 to at a targeted depth of 15 million read-pairs

230 per sample yielding a total of at least 290 million read-pairs. Raw sequencing data

231 generated by this project was deposited in the European Nucleotide Archive under

232 Bioproject PRJEB25137.

233

234 **Differential gene expression and transcript usage analysis**

235

236 Reads were adapter and quality trimmed with Cutadapt (version 1.16, options: -q 15

237 --trim-n -m 36) (Martin, 2011) and then Trimmommatic (version 0.36, default options)

238 (Bolger, Lohse, & Usadel, 2014) to remove remaining residual adapter sequence.

239 Fastq files were inspected using FastQC (Andrews, 2010) before and after quality

240 filtering to confirm the removal of adapter-derived and low-quality sequences and

241 reports combined using multiQC (versions 1.8). We used a transcript-driven

242 approach to quantify gene expression as (1) an excellent gene-set is available for *D.*

243 *magna* (Orsini et al., 2016, 2018), (2) 'alignment-free' mapping approaches to

244 transcripts are at least the equal of genome-based alignments for RNASeq (C.

245 Zhang, Zhang, Lin, & Zhao, 2017), and (3) the *D. magn*a genome is still in draft form

246 with many genes overlapping and/or spread across multiple scaffolds. Gene

247 expression per replicate was quantified using Salmon v0.13.1 (Patro, Duggal, Love,

248 Irizarry, & Kingsford, 2017) with parameters "salmon quant --dumpEq --

249   validateMappings --rangeFactorizationBins 4 -l A --seqBias –gcBias" against the *D. magna*

250   reference transcriptome (Orsini et al., 2016, 2018). The reference transcriptome was

251   created by combining principal and alternative transcripts (downloaded from

252   http://arthropods.eugenes.org/EvidentialGene/daphnia/daphnia_magna/Genes/early

253   access) and indexed with a k-mer size of 25.

254

255   The salmon results were converted into a gene-by-replicate expression matrix for

256   input to DESeq2 (Love, Huber, & Anders, 2014) with the R package tximport

257   (Soneson, Love, & Robinson, 2015). Read mapping rates per replicate were taken

258   from the resulting Salmon log files (Supplementary Table S1). Differential gene

259   expression between caloric restriction and normal food replicates was tested using

260   DESeq2, with 'mother' fit as a blocking factor (~ mother + condition). We

261   incorporated log_2-fold changes into our significance test and report genes significant

262   at log_2-fold change thresholds of 1, and 2 as this is more robust than post-hoc

263   filtering of genes by log_2-fold change alone. This method results in s-values for the

264   non-zero log_2-fold change analyses (i.e log_2-fold change 1 and 2) which are

265   analogous to q-values (Stephens, 2016; Zhu, Ibrahim, & Love, 2019). S-values are a

266   measure of the chance that the sign (+ or -) of the log_2-fold change for the gene is

267   question is incorrect. We applied a significance threshold of 0.005 to the s-values as

268   recommended by DESeq2 and apeglm (Zhu et al., 2019) package authors, as s-

269   values are less conservative than q-values. We also performed significance testing

270   without imposing a log_2-fold change threshold (referred to as 0 log_2-fold change) in

271   DESeq2, with a q-value threshold of 0.05. We advise caution on the use of log_2-fold

272   change thresholds, however. Although they helped us to identify a general trend in

273   the data, the method penalised high expression genes. This is because the variance

274   in gene-expression increases with the level of gene expression, meaning that high-

275   expression genes have wider confidence intervals on their predicted $\log_2$-fold

276   changes. Therefore, we also considered genes differentially expressed at $\log_2$-fold

277   change 0 with overall expression of greater than 10,000 length-scaled transcript per

278   million (TPM) when interpreting the results. Differential transcript usage (DTU) was

279   tested in DRIMSeq (Nowicka & Robinson, 2016) and DEXSeq (Anders, Reyes, &

280   Huber, 2012) and the overall false discovery rate (OFDR) for a two-step procedure

281   (here referring to gene- and transcript-level) was calculated in stageR following

282   (Love, Soneson, & Patro, 2018), with 'mother' fit as a blocking factor as for DESeq2.

283   Only those genes that exhibited significant DTU in both DRIMSeq and DEXSeq after

284   OFDR were considered further. Differential gene and transcript usage scripts are

285   given in Supplementary File S1.

286

287   **TopGO and gene set enrichment analysis**

288

289   Gene ontology term enrichment was tested in topGO (Alexa & Rahnenfuhrer, 2016)

290   for each category of significant gene from gene- and transcript-level analyses using

291   *D. magna* GO term annotations following (Hearn et al., 2018; Hearn, Pearson, et al.,

292   2019). A conservative p-value threshold of 0.01 was applied with no multiple testing

293   correction in line with topGO author recommendation (Section 6.2. The adjustment of

294   p-values, topGO manual: https://bioconductor.org/packages/release/bioc/html/topGO.html).

295   We considered enriched GO terms of the biological process (BP) and molecular

296   function (MF) sub-categories for discussion. We clustered the significantly enriched

297   GO terms in two-dimensional semantic space and treemaps of higher-order

298   processes using REVIGO (Supek, Bošnjak, Škunca, & Šmuc, 2011) following

299   (Hearn, Blaxter, et al., 2019) to identify patterns in enrichment and reduce

300   redundancy in GO terms. We adapted the REVIGO webserver-produced R-script for

301   each category of enriched GO terms to combine groups of terms by colour according

302   to the REVIGO treemap categories (R script, Supplementary File S1).

303

304   Gene set enrichment analysis (GSEA) of *D. magna* KEGG (Kyoto Encyclopedia of

305   Genes and Genomes) orthologs (Kanehisa & Goto, 2000; Kanehisa, Sato,

306   Kawashima, Furumichi, & Tanabe, 2015) was applied to identify KEGG gene

307   pathways up- or down-regulated under CR. GSEA was run for all genes in the

308   expression experiment using their $\log_2$-fold changes from the $\log_2$-fold change zero

309   differential gene expression experiment. To obtain KEGG annotations for each gene

310   the *D. magna* gene-set was annotated with trinotate (Haas et al., 2013) and gene-to-

311   KEGG annotations were input to the universal enrichment protocol of clusterProfiler

312   (Yu, Wang, Han, & He, 2012), a q-value cut-off of 0.05 was used to determine

313   significance (R scripts: Supplementary File S1). We ran 1000 iterations of GSEA as

314   the results were variable between runs and selected only those KEGG terms found

315   significant in >95% of runs.

316

317   **Interaction between expression level and differential methylation**

318

319   Average TPM gene expressions calculated in tximport and normalised in DESeq for

320   CR and NF were correlated with the proportion of methylation within genes for the

321   corresponding treatment using data taken from Hearn, Pearson, et al., (2019).

322   Proportion methylated was defined as the count of methylated reads over the total

323   reads at CpG sites within a genic region (exons + introns) aligned against from the

324　*D. magna* genome assembly (version 2.4) using Bismark (Krueger & Andrews,

325　2011), see Hearn, Pearson, et al., (2019) for further detail. Genic regions were

326　defined from the *D. magna* reference annotation (downloaded from

327　http://arthropods.eugenes.org/EvidentialGene/daphnia/daphnia_magna/Genes/early

328　access/dmagset7finloc9c.puban.gff.gz). CpG counts for CR or NF were extracted by

329　combining CpG counts of the six replicates per treatment from Hearn, Pearson, et

330　al., (2019) from Bismark bam files. Average methylation rates within genic regions

331　per treatment were calculated using bedtools (Quinlan & Hall, 2010). We then

332　combined CpG averages with corresponding average TPM expression for each

333　gene, calculated from the normalised Salmon count matrix. Genes that had

334　expression greater than 10 TPM, at least 5% CpG methylation, and did not overlap

335　another gene in *D. magna* annotation were retained for the correlation analysis. We

336　applied Spearman's rho and Kendall's tau calculated in base R to the results,

337　because of the lack of normality in the proportions of methylation and mean

338　expression data. Furthermore, we intersected the list of differentially expressed

339　genes at each $\log_2$-fold threshold and differential transcript usage with the

340　differentially-methylated regions identified in response to CR from Hearn, Pearson,

341　et al., (2019).

342

343　**miRNA target prediction and mRNA-miRNA expression correlation**

344

345　MiRNA targets of differentially expressed miRNAs identified in Hearn et al., (2018)

346　were predicted in the 3' untranslated regions (3' UTRs, following Graham & Barreto,

347　2019) of differentially expressed genes using PITA (Kertesz, Iovino, Unnerstall, Gaul,

348　& Segal, 2007), RNAhybrid (Krüger & Rehmsmeier, 2006), miRanda (Enright et al.,

349 2003), MicroTar (Thadani & Tammi, 2006) and rna22 (Miranda et al., 2006)

350 implemented on the tools4miRs platform (Lukasik, Wójcikowski, & Zielenkiewicz,

351 2016). Only those 3' UTRs predicted as targets by at least four programs were

352 considered further. Pearson's correlation performed in miRLAB (Le, Zhang, Liu, Liu,

353 & Li, 2015). The DESeq2 normalised count matrices for differentially expressed

354 miRNAs from (Hearn et al., 2018) and mRNAs at $\log_2$-fold change 0 were supplied

355 as input to miRLAB, and the results were intersected with the list of predicted miRNA

356 to mRNA targets. MiRNA-mRNA pairs with greater than 0.5 or less than -0.5

357 correlation in expression level were considered further.

358

359 **Results**

360

361 **Effect of CR on longevity**

362 Cox's proportional hazards ANOVA (see Supplementary File S1 for R code and

363 model output) of the survivorship data (Supplementary File S2) showed that CR *D.*

364 *magna* lived longer on average than NF *D. magna* ($\chi2 = 13.26$, p = 0.0003; Figure 1,

365 part A). Clone 32 was one of the clones that demonstrated increased longevity under

366 CR (Figure 1, Part B). Genotypes also differed in their lifespans ($\chi2 = 155.4$, p <

367 0.0001), and there was a significant interaction between genotype and food level for

368 differences in longevity (Figure 1; $\chi2 = 29.4$, p = 0.0001).

369 **Expression experiment**

370

371 A median of 23,365,302 read-pairs were sequenced per sample with a range of

372 21,452,900-26,752,873, and FastQC revealed no issues with read quality after

373   trimming (Supplementary Table S1: read filtering and alignment rates,

374   Supplementary File S3: multiQC report). Read mapping rates of greater than 80%

375   were recorded for all replicates, except one (3H2, normal food) that had a mapping

376   rate of 74% (Supplementary Table S1). Similar differences in gene expression occur

377   at the 0 log_2-fold change analysis at 3345 up-regulated and 3064 down-regulated

378   under CR (Table 1, Supplementary Tables S2-S4). This global response was

379   reflected in principal components analysis of replicates (Figure 2), in which the first

380   component explains 49% of the variance and separates all sample pairs by

381   treatment. This was also true for miRNAs derived from the same RNA extractions

382   (Hearn et al., 2018). However, with increasing log_2-fold change thresholds there was

383   a bias towards genes being up-regulated in CR (Table 1).

384

385   There were 75 genes with a mean expression greater than 10,000 TPM that were

386   significant at the log_2-fold change 0 threshold up-regulated in CR, versus 15 that

387   were down-regulated. Four of the 15 genes down-regulated under CR were super-

388   oxide dismutases, including the most expressed gene (Dapma7bEVm009708) at a

389   mean expression of 847468.627 TPM. This was over 6-fold greater than the next

390   gene, a Vitellogenin-1 precursor (Dapma7bEVm014991) (Supplementary Table S5:

391   gene descriptions and expression levels). Two further Vitellogenin-1 precursor

392   genes were in the top five most expressed genes (Dapma7bEVm018415 and

393   Dapma7bEVm029595), as was a di-domain hemoglobin precursor

394   (Dapma7bEVm029622). By contrast, the gene lists for the log_2-fold changes 1 and

395   2 were composed of genes at relatively modest expression levels and contained a

396   high proportion of uncharacterised genes (Supplementary Table S5).

397

Differential Transcript Usage and Hb related genes

For differential transcript usage, 498 transcripts corresponding to 294 genes were significant in the DEXSeq analysis and 327 transcripts from 187 genes for the DRIMSeq analysis. There was an overlap of 181 transcripts and 112 genes between the two methods (Supplementary File S4: DRIMSeq transcript expression levels for DTU significant genes). Of these, 32 genes have a mean gene expression normalised count level greater than 1000 TPM and five greater than 10000 TPM. The most highly-expressed DTU exhibiting gene was a di-domain haemoglobin precursor (Figure 3, Dapma7bEVm014981) with a TPM of 65,675. The isoform most abundant in CR replicates ("transcript 21", Figure 3) does not contain an erythrocruorin domain, whereas an isoform containing three such domains ("transcript 12", Figure 3), is down-regulated in CR. A further di-domain haemoglobin was also in this high expression group (Dapma7bEVm015367, TPM 13,532). Other notable examples of DTU included a Neurocalcin in which transcript 2 is heavily up-regulated in CR (Supplementary File S4: Dapma7bEVm018721), a Carboxypeptidase A4 (Dapma7bEVm015011), a Lactosylceramide (Dapma7bEVm007442), and an Ezrin-moesin-radixin (Dapma7bEVm009772).

Following from this result we found that one Hb trans-inducer HIF-1α (Dapma7bEVm009543) was up-regulated significantly in CR ($\log_2$-fold change 0) at a mean expression of 6903 TPM versus 4558 in NF. Three of the HIF-1 co-dimer HIF-1β genes were DE at this threshold, the highest expressed gene was down-regulated in CR at a mean 2316 TPM versus 2667 in NF. The two other HIF-1β genes were up-regulated in CR, but had lower in average overall expression at 464

423   and 391 TPM respectively. An mTOR protein kinase (Dapma7bEVm000341) was

424   also up-regulated under CR at log_2-fold change 0 albeit with a modest log_2-fold

425   change overall (0.14) and mean expression of 2434 TPM.

426

427   **Gene ontology and gene set enrichment analyses**

428

429   For molecular function GO term enrichment approximately equal numbers of terms

430   at 20 and 21 significant terms up- and down-regulated at log_2-fold change 0

431   respectively (Supplementary Table S6). Biological process GO terms differ in that 25

432   terms are enriched for genes down-regulated in CR at log_2-fold change 0, versus 8

433   that were up-regulated (REVIGO clustering of GO terms, Figure 4 and

434   Supplementary Table S7).

435

436   For the GSEA analysis of KEGG terms, five of the six enriched terms that occur in at

437   least 95% of 1000 iterations were groups of genes up-regulated under CR

438   (representative GSEA result, Figure 5). The five KEGG terms significantly enriched

439   in CR were for serine/threonine-protein kinase/endoribonuclease IRE1 (K08852),

440   preprotein translocase subunit SecA (K03070), serine/threonine-protein

441   kinase/endoribonuclease IRE2 (K11715), chitinase (K01183) and cytochrome P450

442   family 4 (K15001). The single term enriched under normal food was for

443   apolipoprotein D and lipocalin family protein (K03098).

444

445   **Overlap with differentially methylated regions**

446

447 Over 2000 genes that met our criteria (i.e., expression greater than 10 and at least

448 5% methylation) were included in the correlations with CpG methylation rate for each

449 of the NF and CR comparisons. Weak, significant and highly-concordant negative

450 correlations were found for both comparisons for Kendall's tau and Spearman's rho

451 (Supplementary File S5). Previously we identified 115 and 192 genes containing

452 regions of hypo- or hypermethylated at CpG sites under CR respectively (Hearn,

453 Pearson, et al., 2019). For both categories of methylation there was little signal of co-

454 regulation with gene-expression. The majority of overlap occurs at the $\log_2$-fold 0

455 level for which thousands of genes were significantly up- and down-regulated under

456 CR implying a high-degree of overlap by chance (Table 2). Only two genes up-

457 regulated in CR with a $\log_2$-fold change of 1 or greater intersected with differentially

458 methylated regions. One was an uncharacterised gene (Dapma7bEVm028334)

459 which was identified as hypo-methylated under CR in Hearn, Pearson, et al., (2019),

460 and the other an integral membrane protein (Dapma7bEVm027395) which was

461 hyper-methylated under CR.

462

463 **miRNA interaction**

464

465 In total 240 miRNA-mRNA pairs were predicted by the combined target-site method,

466 which was composed of 117 genes and 34 miRNAs (miRNA-mRNA pairs and

467 miRbase homologs: Supplementary Table S8). Many miRNAs were predicted by our

468 combined approach to target multiple genes, hence the discrepancy between

469 number of genes and miRNAS. As for the expression analyses these miRNA-mRNA

470 pairs showed a bias toward genes expressed more highly under CR (Table 3). The

471 strongest negative correlation for genes up-regulated in CR was -0.71 and the

472   strongest positive correlation was 0.87. There was little overlap between these

473   genes and other genes of interest, but a Histone-lysine N-methyltransferase Suv4-20

474   (Dapma7bEVm018601, mean expression = 10277 TPM) up-regulated under CR had

475   a negative correlation with nine miRNAs (Supplementary Table S8: gene description

476   for gene numbers included in Table 3). Four of the genes exhibiting DTU were

477   predicted to have miRNA targets, of these only a Para-nitrobenzyl esterase

478   (Dapma7bEVm000405), was annotated.

479

480   **Discussion**

481

482   Firstly, We established that CR has an effect on average lifespan across eight

483   different genotypes of *D. magna*, in line with previous results (Garbutt & Little, 2014,

484   2017; Latta IV et al., 2011). Focussing on Clone 32 we explored the molecular basis

485   of CR through difference in gene expression with normal food levels. This difference

486   was global, as over 6000 genes respond to treatment (Table 1. Log-fold change 0).

487   Differential methylation identified previously in response to CR in Clone 32 (Hearn,

488   Pearson, et al., 2019) did not impact upon gene expression. The abundance of

489   several miRNAs that respond to CR in Clone 32 (Hearn et al., 2018) correlated with

490   gene expression, and these correlations were biased towards higher expression in

491   the CR treatment. Generally, we showed that more genes are significantly up-

492   regulated under CR (Table 1) and for the remainder of the discussion we focus on

493   the responses of particular genes and pathways to CR.

494

495   **A haemoglobin response to CR in *D. magna***

496

497 Fewer genes had differential transcript usage detected than differential gene
498 expression. This may reflect biological reality as the eight replicates per condition
499 give reasonable power in DTU analyses (by comparison to simulated data in Love et
500 al., 2018). Alternatively, this may be because we were conservative in our approach
501 to filtering DTUs by only taking the union of DEXSeq and DRIMSeq. Gene isoforms
502 may also be under-annotated, however the gene-set used as a reference results
503 from a comprehensive bioinformatic construction after exposure of *D. magna* to
504 twelve environmental stressors (Orsini et al., 2016).

505

506 DTU analysis identified a highly-expressed Hb gene that responded to CR by
507 changing isoform proportions (Figure 3). We believe it is the first time haemoglobin
508 genes have been implicated in CR in *D. magna*. This is concordant with the
509 observed changing Hb protein levels in response to food (Fox et al., 1951). The gene
510 involved, Dapma7bEVm014981, has many different isoforms with the three most
511 highly expressed in this experiment exhibiting varied proportions of expression
512 between CR and NF. Most strikingly, transcript 12, which encodes three
513 erythrocruorin (IPR002336) domains, occurs at much higher expression in NF than
514 CR (Figure 3). These erythrocruorin domain provides the scaffold for a Haem-
515 binding pocket (http://www.ebi.ac.uk/interpro/entry/InterPro/IPR002336/) and hence
516 oxygen affinity of the haemoglobin gene-product. Based on these results we
517 hypothesise that *D. magna* moderates its haemoglobin mix in response to CR by
518 reducing respiration leading to a lower proportion of haemoglobin containing
519 erythrocruorin domains under CR. This is evidenced by a change in the proportions
520 of expressed isoforms of gene Dapma7bEVm014981 under CR in favour of isoforms
521 without (transcript 21) an erythrocruorin domain or two domains only (transcript 11).

522 Thus variation in erythrocruorin domains could underly the observed correlation

523 between oxygen-binding capacity and structurally distinct Hb-gene isoforms (Zeis,

524 2020). Future studies of Hb response to environmental stressors in *Daphnia* should

525 consider differential isoform as well as Hb gene-copy usage following our insights

526 here.

527

528 The Hb mix of *D. magna* is known to change in response to hypoxia due to the

529 action of the dimeric hypoxia-inducible factor 1 (Cuenca Cambronero et al., 2018;

530 Zeis, 2020). We identified that the HIF-1α component of the Hb gene transcription

531 factor HIF-1 is up-regulated in CR, as are two HIF-1β genes. However, the most

532 highly-expressed HIF-1β is down-regulated in CR. The discordant patterns of HIF-1

533 component expression suggests HIF-1 regulation is not straightforward. Indeed, in *C.*

534 *elegans* HIF-1 can promote or limit longevity (Leiser & Kaeberlein, 2010). The

535 involvement of HIF-1 suggests a previously unidentified overlap in hypoxia and CR

536 response in *Daphnia*. This may explain the similar phenotypic effects on body size in

537 offspring under hypoxia and CR, with little associated impact on reproduction of CR

538 and hypoxia (Garbutt & Little, 2017; Hearn et al., 2018; Seidl et al., 2005). It also

539 indicates that the mTOR pathway is active in the *D. magna* response to CR (Land &

540 Tee, 2007), which was supported here by up-regulation under CR of an mTOR

541 protein kinase (Dapma7bEVm000341). An alternative to the HIF-1 induction pathway

542 exists and it is triggered by juvenile hormone (Rider, Gorr, Olmstead, Wasilak, &

543 LeBlanc, 2005). We did not see evidence for juvenile hormone involvement in the

544 gene expression results, although this would require hormone assays to discard

545 rigorously.

546

The endoplasmic reticulum stress response under CR

The serine/threonine-protein kinase/endoribonuclease inositol-requiring enzyme 1 KEGG category (IRE1, K08852) was up-regulated under CR in clusterProfiler GSEA analysis (Figure 5). IRE1 is a sensor protein in the unfolded protein response (UPR) that lowers stress in the endoplasmic reticulum. When activated it initiates a transcription factor (X-box binding protein 1) that up-regulates endoplasmic reticulum associated degradation genes (ERAD) (Calfon et al., 2002). HIF-1 mediated CR lifespan increases in *C. elegans* depends on IRE1 (Di Chen & Kapahi, 2009). Transient CR-derived stress in *C. elegans* larvae causes a robust IRE1-dependent UPR to be maintained into adulthood, which is an example of hormesis (Matai et al., 2019). The up-regulation of IRE1 reported here links the CR response in *D. magna* to protein homeostasis in the ER, the dysregulation of which is strongly linked to ageing in general (Brown et al., 2014; Chadwick & Lajoie, 2019; Cohen, Bieschke, Perciavalle, Kelly, & Dillin, 2006; Steinkraus et al., 2008). This gene has further roles in CR in other organisms. It regulates the increased usage of intestinal triacyglycerol in *Drosophila* which mediates the metabolic adaptation of midgut epithelium to CR (Luis et al., 2016). While in mice the upregulation of IRE1 in response to a reduced protein diet protects against cancer (Rubio-Patiño et al., 2018).

Superoxide dismutase was down-regulated under CR

Several of the well-known candidate response genes to CR were significantly up-regulated under CR, including sirtuins, IGF, and the mTOR protein kinase. None of these genes showed large differences in their mean expression and $\log_2$-fold changes were modest.

571

572 Copper-zinc super-oxide dismutase (SOD) was down-regulated under CR in *D.*

573 *magna,* it also showed varying responses to CR (or links to longevity) in other

574 systems such as yeast (Mesquita et al., 2010). Over-expression of copper-zinc and

575 manganese SOD in *Drosophila* did not increase lifespan (Orr, Mockett, Benes, &

576 Sohal, 2003), and in termites increased longevity of queens was associated with

577 enzyme activity and not expression level (Tasaki, Kobayashi, Matsuura, & Iuchi,

578 2018). The effect of SOD disruption on lifespan varies by experimental context in

579 *Drosophila* (Wang, Branicky, Noë, & Hekimi, 2018). In *D. magna* copper-zinc SOD is

580 known to increase in expression in response to copper, ammonia, and hypoxia levels

581 as they are considered to be general stress-response factors (Lyu, Zhu, Wang,

582 Chen, & Yang, 2013). We hypothesise that up-regulated SOD production under NF

583 was due to greater ROS production from higher-respiration levels than CR which

584 was compensated for by greater SOD expression. An alternative explanation is that

585 dissolved oxygen content was lowered in NF rearing jars by increased respiration-

586 levels versus CR jars leading to a hypoxia-induced stress-response known to occur

587 in *D. magna* and *D. pulex* in low oxygen conditions (Klumpen et al., 2017; Lyu et al.,

588 2013). This could also explain the Dapma7bEVm014981 Hb gene expressing

589 differential transcripts in response to hypoxia through oxygen-depletion in NF versus

590 CR.

591

592 **Several processes were repressed under CR**

593

594 Guanosine triphosphate (GTP) related molecular function GO terms dominated

595 enrichment in genes down-regulated under CR. The down-regulation of a GTPase

596   has a key role in life-extension due to CR in *C. elegans* (Hansen et al., 2008). This is

597   hypothesized to stimulate recycling organelles and cytoplasmic proteins (autophagy),

598   which promotes increased lifespans through down-stream mechanisms (Hansen et

599   al., 2008).

600

601   Apolipoprotein D and other lipocalin genes (K03098) were down-regulated under

602   CR. In *Drosophila* overexpression of Apolipoprotein D increased lifespan by 18%

603   and tolerance to starvation, and could act as a scavenger of toxic products in

604   defence against oxidative stress (Sanchez et al., 2006; Walker, Muffat, Rundel, &

605   Benzer, 2006). Why this class of genes would be reduced in expression under CR in

606   *D. magna* rather than up-regulated is unclear. Perhaps NF individuals are more

607   developmentally advanced due to their rapid growth than CR individuals and are

608   combating the effects of accumulated oxidative stress earlier in life.

609

610   **A weak correlation between gene methylation and expression**

611

612   We observed a negative correlation between genes with a methylated CpG portion

613   greater than 5% and gene expression. The highly concordant results for CR and NF

614   comparisons indicate there is no effect of CR on this relationship. In *D. magna,* links

615   between methylation and alternative splicing have been observed previously

616   (Asselman et al., 2017; Kvist et al., 2018) and DNA methylation is enriched in gene-

617   bodies. We saw no overlap between the DTU analysis and previously identified

618   genes overlapping differentially methylated regions (DMRs), which is perhaps not

619   surprising given the expression-methylation correlations between CR and NF

620   expression and CpG methylation are essentially the same. These results contrast

621   with (Kvist et al., 2018) in which methylation at exons two to four exhibits significant

622   positive correlations with gene expression in *D. magna*. Our focus on the response

623   to a treatment differs form Kvist et al., (2018) which defined the evolutionary

624   conservation of methylation across gene bodies in *D. magna*.

625

626   **miRNA correlations are biased towards CR**

627   A robust miRNA response was observed to CR in Hearn et al., (2018) originating

628   from the same total RNA samples included in this study. Here we observed greater

629   miRNA targeting of genes up-regulated in CR at log_2-fold change 0 for both positive

630   and negative correlations (33 in each case, Table 3). This is in keeping with the

631   general bias towards up-regulation in CR across this experiment; we do not see

632   overlap in the miRNA correlated gene-lists with Hb-related genes or SOD discussed

633   above. Of note, there is a negative correlation between nine miRNAs and Histone-

634   lysine N-methyltransferase Suv4-20 (Dapma7bEVm018601). This gene is

635   significantly up-regulated at log_2-fold change 1 under CR (average TPM 15063

636   versus 5278 in NF). Suv4-20 trimethylates histone H4 lysine 20 and has an

637   important role in DNA repair and genomic stability (Jørgensen, Schotta, & Sørensen,

638   2013). However, we must interpret the results with caution as computational miRNA-

639   mRNA target inference is prone to false-positives (Fridrich, Hazan, & Moran, 2019;

640   Pinzón et al., 2017). This is because animal miRNA seed binding is 'wobbly' and

641   does not require perfect complementarity between miRNA and mRNA. Because of

642   this, Fridrich et al., (2019) recommend biological interpretation only when further

643   experimental support is available. This included when taking the overlap of multiple

644   prediction programs as we have done.

645   Demonstrating that an mRNA is regulated by specific miRNAs will require the

646   development of a crosslinking, ligation and sequencing of hybrids (CLASH) protocol

647   for the *D. magna* Argonaute (AGO) proteins (Helwak, Kudla, Dudnakova, &

648   Tollervey, 2013). The CLASH method isolates the AGO-miRNA-mRNA complexes

649   that form during mRNA silencing by miRNA. Sequencing of the interacting RNA in

650   the AGO protein can then be used to identify which miRNAs are bound to what

651   mRNAs under the experimental condition surveyed. Even if the link between miRNA

652   targeting and Suv4-20 is not borne out in future such experiments, the differential

653   expression result indicates a potential link between CR, the histone epigenome, and

654   DNA repair.

655   **Conclusions**

656   We first showed that caloric restriction increases the lifespan of *D. magna* across

657   multiple genotypes. We then chose a CR-responsive genotype to survey the

658   transcriptome of young-adults after their first clutch and detected a number of

659   canonical stress- and CR responses. By contrasting differential transcript usage

660   between CR and NF we also showed that the haemoglobin isoform mix of a highly-

661   expressed *D. magna* Hb gene is reduced for isoforms containing erythrocruorin

662   domains. We speculate that this may reduce the overall respiration-levels of CR

663   individuals and partially explain the observed increased lifespan under CR.

664   Components of the transcription factor that controls Hb-gene transcription, HIF-1, are

665   also differentially expressed linking the response to hypoxia with that for CR. An

666   mTOR protein kinase is also differentially expressed and is known to modulate HIF-

667   1. The mTOR pathway is implicated in CR responses of diverse organisms, which is

668   also the case in *D. magn*a. Future work should test if respiration is depressed under

669 CR through changes to the haemoglobin mix in *D. magna*, and if this response is

670 conserved in non-aquatic organisms.

671 **Acknowledgements**

675 **References**

676 [dataset]Hearn, J., Clark, J., Wilson, P.J., & Little, T.J.; 2019; Differential expression
677 in response to caloric restriction in *Daphnia magna*; European Nucleotide Archive;
678 PRJEB25137.
679
680 Alexa, A., & Rahnenfuhrer, J. (2016). topGO: Enrichment Analysis for Gene
681 Ontology. Available at:
682 https://bioconductor.org/packages/release/bioc/html/topGO.html.
683 Anders, S., Reyes, A., & Huber, W. (2012). Detecting differential usage of exons
684 from RNA-seq data. *Genome Res*, *22*. doi:10.1101/gr.133744.111
685 Andrews, S. (2010). FastQC: A quality control application for high throughput
686 sequence data. Available at:
687 http://www.bioinformatics.babraham.ac.uk/projects/fastqc.
688 Asselman, J., Coninck, D. I. M. De, Beert, E., Janssen, C. R., Orsini, L., Pfrender, M.
689 E., … Schamphelaere, K. A. C. De. (2017). Bisulfite Sequencing with *Daphnia*
690 Highlights a Role for Epigenetics in Regulating Stress Response to Microcystis
691 through Preferential Differential Methylation of Serine and Threonine Amino
692 Acids. *Environmental Science & Technology*, *51*(2), 924–931.
693 doi:10.1021/acs.est.6b03870
694 Auld, S. K. J. R., Hall, S. R., Housley Ochs, J., Sebastian, M., & Duffy, M. A. (2014).
695 Predators and patterns of within-host growth can mediate both among-host
696 competition and evolution of transmission potential of parasites. *The American*
697 *Naturalist*, *184*(S1), S77–S90.
698 Boersma, M., Spaak, P., & De Meester, L. (1998). Predator-mediated plasticity in
699 morphology, life history, and behavior of *Daphnia*: the uncoupling of responses.
700 *The American Naturalist*, *152*(2), 237–248.
701 Bolger, A. M., Lohse, M., & Usadel, B. (2014). Trimmomatic: A flexible trimmer for
702 Illumina sequence data. *Bioinformatics*, *30*(15), 2114–2120.
703 doi:10.1093/bioinformatics/btu170
704 Brown, M. K., Chan, M. T., Zimmerman, J. E., Pack, A. I., Jackson, N. E., & Naidoo,
705 N. (2014). Aging induced endoplasmic reticulum stress alters sleep and sleep
706 homeostasis. *Neurobiology of Aging, 35*(6), 1431–1441.
707 doi:10.1016/j.neurobiolaging.2013.12.005

708   Calfon, M., Zeng, H., Urano, F., Till, J. H., Hubbard, S. R., Harding, H. P., … Ron, D.
709   (2002). IRE1 couples endoplasmic reticulum load to secretory capacity by
710   processing the XBP-1 mRNA. *Nature*, *415*(6867), 92–96.
711   Chadwick, S. R., & Lajoie, P. (2019). Endoplasmic Reticulum Stress Coping
712   Mechanisms and Lifespan Regulation in Health and Diseases. *Frontiers in Cell
713   and Developmental Biology*, *7*, 84. doi:10.3389/fcell.2019.00084
714   Choi, K.-M., Hong, S.-J., van Deursen, J. M., Kim, S., Kim, K. H., & Lee, C.-K.
715   (2018). Caloric restriction and rapamycin differentially alter energy metabolism
716   in yeast. *The Journals of Gerontology: Series A*, *73*(1), 29–38.
717   Cohen, E., Bieschke, J., Perciavalle, R. M., Kelly, J. W., & Dillin, A. (2006). Opposing
718   activities protect against age-onset proteotoxicity. *Science*, *313*(5793), 1604–
719   1610.
720   Colbourne, J. K., Pfrender, M. E., Gilbert, D., Thomas, W. K., Tucker, A., Oakley, T.
721   H., … others. (2011). The ecoresponsive genome of *Daphnia pulex*. *Science*,
722   *331*(6017), 555–561.
723   Cuenca Cambronero, M., Zeis, B., & Orsini, L. (2018). Haemoglobin-mediated
724   response to hyper-thermal stress in the keystone species *Daphnia magna*.
725   *Evolutionary Applications*, *11*(1), 112–120.
726   Di Chen, E. L. T., & Kapahi, P. (2009). HIF-1 modulates dietary restriction-mediated
727   lifespan extension via IRE-1 in *Caenorhabditis elegans*. *PLoS Genetics*, *5*(5).
728   Ding, F., Gil, M. P., Franklin, M., Ferreira, J., Tatar, M., Helfand, S. L., & Neretti, N.
729   (2014). Transcriptional response to dietary restriction in *Drosophila
730   melanogaster*. *Journal of Insect Physiology*, *69*(C), 101–106.
731   doi:10.1016/j.jinsphys.2014.05.002
732   Dobson, A. J., He, X., Blanc, E., Bolukbasi, E., Feseha, Y., Yang, M., & Piper, M. D.
733   W. (2018). Tissue-specific transcriptome profiling of *Drosophila* reveals roles for
734   GATA transcription factors in longevity by dietary restriction. *Npj Aging and
735   Mechanisms of Disease*, *4*(1), 5. doi:10.1038/s41514-018-0024-4
736   Enright, A. J., John, B., Gaul, U., Tuschl, T., Sander, C., & Marks, D. S. (2003).
737   MicroRNA targets in *Drosophila*. *Genome Biology*, *5*(1), R1. doi:10.1186/gb-
738   2003-5-1-r1
739   Fox, H. M., Gilchrist, B. M., & Phear, E. A. (1951). Functions of haemoglobin in
740   *Daphnia*. *Proceedings of the Royal Society of London. Series B-Biological
741   Sciences*, *138*(893), 514–528.
742   Fridrich, A., Hazan, Y., & Moran, Y. (2019). Too Many False Targets for MicroRNAs:
743   Challenges and Pitfalls in Prediction of miRNA Targets and Their Gene
744   Ontology in Model and Non-model Organisms. *Bioessays*, *41*(4), 1800169.
745   Garbutt, J. S., & Little, T. J. (2014). Maternal food quantity affects offspring feeding
746   rate in *Daphnia magna*. *Biology Letters*, *10*(7), 20140356.
747   Garbutt, J. S., & Little, T. J. (2017). Bigger is better: changes in body size explain a
748   maternal effect of food on offspring disease resistance. *Ecology and Evolution*,
749   *7*(5), 1403–1409.
750   Gerke, P., Börding, C., Zeis, B., & Paul, R. J. (2011). Adaptive haemoglobin gene
751   control in *Daphnia pulex* at different oxygen and temperature conditions.
752   *Comparative Biochemistry and Physiology Part A: Molecular & Integrative
753   Physiology*, *159*(1), 56–65.
754   Gladyshev, V. N. (2014). The free radical theory of aging is dead. Long live the
755   damage theory! *Antioxidants & Redox Signaling*, *20*(4), 727–731.
756   doi:10.1089/ars.2013.5228
757   Gorr, T. A., Cahn, J. D., Yamagata, H., & Bunn, H. F. (2004). Hypoxia-induced

758 synthesis of hemoglobin in the crustacean *Daphnia magna* is hypoxia-inducible
759 factor-dependent. *Journal of Biological Chemistry*, *279*(34), 36038–36047.
760 Graham, A. M., & Barreto, F. S. (2019). Novel microRNAs are associated with
761 population divergence in transcriptional response to thermal stress in an
762 intertidal copepod. *Molecular Ecology*, *28*(3), 584–599.
763 Haas, B. J., Papanicolaou, A., Yassour, M., Grabherr, M., Blood, P. D., Bowden, J.,
764 … Regev, A. (2013). *De novo* transcript sequence reconstruction from RNA-seq
765 using the Trinity platform for reference generation and analysis. *Nat. Protocols*,
766 *8*(8), 1494–1512.
767 Hansen, M., Chandra, A., Mitic, L. L., Onken, B., Driscoll, M., & Kenyon, C. (2008). A
768 role for autophagy in the extension of lifespan by dietary restriction in *C.
769 elegans*. *PLoS Genetics*, *4*(2), e24.
770 Hearn, J., Blaxter, M., Schönrogge, K., Nieves-Aldrey, J.-L., Pujade-Villar, J.,
771 Huguet, E., … Stone, G. N. (2019). Genomic dissection of an extended
772 phenotype: Oak galling by a cynipid gall wasp. *PLoS Genetics*, *15*(11),
773 e1008398–e1008398. doi:10.1371/journal.pgen.1008398
774 Hearn, J., Chow, F. W.-N., Barton, H., Tung, M., Wilson, P., Blaxter, M., … Little, T.
775 J. (2018). *Daphnia magna* microRNAs respond to nutritional stress and ageing
776 but are not transgenerational. *Molecular Ecology*, *27*(6), 1402–1412.
777 Hearn, J., Pearson, M., Blaxter, M., Wilson, P. J., & Little, T. J. (2019). Genome-wide
778 methylation is modified by caloric restriction in *Daphnia magna*. *BMC Genomics*,
779 *20*(1), 197. doi:10.1186/s12864-019-5578-4
780 Heilbronn, L. K., & Ravussin, E. (2003). Calorie restriction and aging: review of the
781 literature and implications for studies in humans. *The American Journal of
782 Clinical Nutrition*, *78*(3), 361–369.
783 Heintz, C., Doktor, T. K., Lanjuin, A., Escoubas, C., Zhang, Y., Weir, H. J., … Mair,
784 W. B. (2017). Splicing factor 1 modulates dietary restriction and TORC1
785 pathway longevity in *C. elegans*. *Nature*, *541*(7635), 102–106.
786 doi:10.1038/nature20789
787 Helwak, A., Kudla, G., Dudnakova, T., & Tollervey, D. (2013). Mapping the human
788 miRNA interactome by CLASH reveals frequent noncanonical binding. *Cell*,
789 *153*(3), 654–665.
790 Johnson, S. C., Rabinovitch, P. S., & Kaeberlein, M. (2013). mTOR is a key
791 modulator of ageing and age-related disease. *Nature*, *493*(7432), 338–345.
792 doi:10.1038/nature11861
793 Jørgensen, S., Schotta, G., & Sørensen, C. S. (2013). Histone H4 lysine 20
794 methylation: key player in epigenetic regulation of genomic integrity. *Nucleic
795 Acids Research*, *41*(5), 2797–2806.
796 Kanehisa, M., & Goto, S. (2000). KEGG: kyoto encyclopedia of genes and genomes.
797 *Nucleic Acids Research*, *28*(1), 27–30.
798 Kanehisa, M., Sato, Y., Kawashima, M., Furumichi, M., & Tanabe, M. (2015). KEGG
799 as a reference resource for gene and protein annotation. *Nucleic Acids
800 Research*, *44*(D1), D457--D462.
801 Kapahi, P., Kaeberlein, M., & Hansen, M. (2017). Dietary restriction and lifespan:
802 Lessons from invertebrate models. *Ageing Research Reviews*, *39*, 3–14.
803 doi:10.1016/j.arr.2016.12.005
804 Kenyon, C. J. (2010). The genetics of ageing. *Nature*, *464*(7288), 504–512.
805 doi:10.1038/nature08980
806 Kertesz, M., Iovino, N., Unnerstall, U., Gaul, U., & Segal, E. (2007). The role of site
807 accessibility in microRNA target recognition. *Nature Genetics*, *39*(10), 1278–

808   1284.

809   Kim, S.-S., Choi, K.-M., Kim, S., Park, T., Cho, I.-C., Lee, J.-W., & Lee, C.-K. (2016).
810   Whole-transcriptome analysis of mouse adipose tissue in response to short-term
811   caloric restriction. *Molecular Genetics and Genomics*, *291*(2), 831–847.
812   doi:10.1007/s00438-015-1150-3

813   Klumpen, E., Hoffschröer, N., Zeis, B., Gigengack, U., Dohmen, E., & Paul, R. J.
814   (2017). Reactive oxygen species (ROS) and the heat stress response of
815   *Daphnia pulex*: ROS-mediated activation of hypoxia-inducible factor 1 (HIF-1)
816   and heat shock factor 1 (HSF-1) and the clustered expression of stress genes.
817   *Biology of the Cell*, *109*(1), 39–64.

818   Koubova, J., & Guarente, L. (2003). How does calorie restriction work? *Genes &*
819   *Development*, *17*(3), 313–321.

820   Krueger, F., & Andrews, S. R. (2011). Bismark: a flexible aligner and methylation
821   caller for Bisulfite-Seq applications. *Bioinformatics*, *27*(11), 1571–1572.

822   Krüger, J., & Rehmsmeier, M. (2006). RNAhybrid: microRNA target prediction easy,
823   fast and flexible. *Nucleic Acids Research*, *34*(suppl_2), W451--W454.

824   Kvist, J., Gonçalves Athanàsio, C., Shams Solari, O., Brown, J. B., Colbourne, J. K.,
825   Pfrender, M. E., & Mirbahai, L. (2018). Pattern of DNA Methylation in *Daphnia*:
826   Evolutionary Perspective. *Genome Biology and Evolution*, *10*(8), 1988–2007.
827   doi:10.1093/gbe/evy155

828   Lai, K.-P., Li, J.-W., Chan, C. Y.-S., Chan, T.-F., Yuen, K. W.-Y., & Chiu, J. M.-Y.
829   (2016). Transcriptomic alterations in *Daphnia magna* embryos from mothers
830   exposed to hypoxia. *Aquatic Toxicology*, *177*, 454–463.

831   Lakowski, B., & Hekimi, S. (1998). The genetics of caloric restriction in
832   *Caenorhabditis elegans*. *Proceedings of the National Academy of Sciences of*
833   *the United States of America*, *95*(22), 13091–13096.
834   doi:10.1073/pnas.95.22.13091

835   Lampert, W. (1987). Feeding and nutrition in *Daphnia*. In R. H. Peters & R. De
836   Bernardi (Eds.), *Daphnia* (p. 502). Men. Ist. Ital. Idrobiol.

837   Land, S. C., & Tee, A. R. (2007). Hypoxia-inducible factor 1α is regulated by the
838   mammalian target of rapamycin (mTOR) via an mTOR signaling motif. *Journal*
839   *of Biological Chemistry*, *282*(28), 20534–20543.

840   Latta IV, L. C., Frederick, S., & Pfrender, M. E. (2011). Diet restriction and life history
841   trade-offs in short-and long-lived species of *Daphnia*. *Journal of Experimental*
842   *Zoology Part A: Ecological Genetics and Physiology*, *315*(10), 610–617.

843   Le, T. D., Zhang, J., Liu, L., Liu, H., & Li, J. (2015). MiRLAB: An R based dry lab for
844   exploring miRNA-mRNA regulatory relationships. *PLoS ONE*, *10*(12), 1–15.
845   doi:10.1371/journal.pone.0145386

846   Lee, S.-J., Hwang, A. B., & Kenyon, C. (2010). Inhibition of respiration extends *C.*
847   *elegans* life span via reactive oxygen species that increase HIF-1 activity.
848   *Current Biology*, *20*(23), 2131–2136.

849   Leiser, S. F., & Kaeberlein, M. (2010). The hypoxia-inducible factor HIF-1 functions
850   as both a positive and negative modulator of aging. *Biological Chemistry*,
851   *391*(10), 1131–1137.

852   Love, M. I., Huber, W., & Anders, S. (2014). Moderated estimation of fold change
853   and dispersion for RNA-seq data with DESeq2. *Genome Biology*, *15*(12), 550.
854   doi:10.1186/s13059-014-0550-8

855   Love, M. I., Soneson, C., & Patro, R. (2018). Swimming downstream: statistical
856   analysis of differential transcript usage following Salmon quantification.
857   *F1000Research*, *7*.

858 Luis, N. M., Wang, L., Ortega, M., Deng, H., Katewa, S. D., Li, P. W.-L., … Kapahi,
859   P. (2016). Intestinal IRE1 is required for increased triglyceride metabolism and
860   longer lifespan under dietary restriction. *Cell Reports*, *17*(5), 1207–1216.
861 Lukasik, A., Wójcikowski, M., & Zielenkiewicz, P. (2016). Tools4miRs – one place to
862   gather all the tools for miRNA analysis. *Bioinformatics*, *32*(17), 2722–2724.
863   doi:10.1093/bioinformatics/btw189
864 Lyu, K., Wang, Q., Li, Z., Chen, R., Zhu, C., Liu, J., & Yang, Z. (2015). Age-
865   dependent survival and selected gene expression in *Daphnia magna* after short-
866   term exposure to low dissolved oxygen. *Journal of Plankton Research*, *37*(1),
867   66–74.
868 Lyu, K., Zhu, X., Wang, Q., Chen, Y., & Yang, Z. (2013). Copper/Zinc Superoxide
869   Dismutase from the Cladoceran *Daphnia magna*: Molecular Cloning and
870   Expression in Response to Different Acute Environmental Stressors.
871   *Environmental Science & Technology*, *47*(15), 8887–8893.
872   doi:10.1021/es4015212
873 Martin, M. (2011). Cutadapt removes adapter sequences from high-throughput
874   sequencing reads. *EMBnet.Journal*, *17*(1).
875 Matai, L., Sarkar, G. C., Chamoli, M., Malik, Y., Kumar, S. S., Rautela, U., …
876   Mukhopadhyay, A. (2019). Dietary restriction improves proteostasis and
877   increases life span through endoplasmic reticulum hormesis. *Proceedings of the
878   National Academy of Sciences*, *116*(35), 17383 LP – 17392.
879   doi:10.1073/pnas.1900055116
880 Matthews, D., Diskin, M. G., Kenny, D. A., Creevey, C. J., Keogh, K., & Waters, S.
881   M. (2017). Effect of short term diet restriction on gene expression in the bovine
882   hypothalamus using next generation RNA sequencing technology. *BMC
883   Genomics*, *18*(1), 1–14. doi:10.1186/s12864-017-4265-6
884 Mesquita, A., Weinberger, M., Silva, A., Sampaio-Marques, B., Almeida, B., Leão,
885   C., … Ludovico, P. (2010). Caloric restriction or catalase inactivation extends
886   yeast chronological lifespan by inducing H_2O_2 and superoxide dismutase
887   activity. *Proceedings of the National Academy of Sciences*, *107*(34), 15123 LP –
888   15128. doi:10.1073/pnas.1004432107
889 Miranda, K. C., Huynh, T., Tay, Y., Ang, Y.-S., Tam, W.-L., Thomson, A. M., …
890   Rigoutsos, I. (2006). A pattern-based method for the identification of MicroRNA
891   binding sites and their corresponding heteroduplexes. *Cell*, *126*(6), 1203–1217.
892 Mitchell, S. E., & Lampert, W. (2000). Temperature adaptation in a geographically
893   widespread zooplankter, *Daphnia magna*. *Journal of Evolutionary Biology*,
894   *13*(3), 371–382.
895 Most, J., Tosti, V., Redman, L. M., & Fontana, L. (2017). Calorie restriction in
896   humans: An update. *Ageing Research Reviews*, *39*, 36–45.
897   doi:10.1016/j.arr.2016.08.005
898 Muid, K. A., Karakaya, H. Ç., & Koc, A. (2014). Absence of superoxide dismutase
899   activity causes nuclear DNA fragmentation during the aging process.
900   *Biochemical and Biophysical Research Communications*, *444*(2), 260–263.
901 Muller, F. L., Song, W., Liu, Y., Chaudhuri, A., Pieke-Dahl, S., Strong, R., … others.
902   (2006). Absence of CuZn superoxide dismutase leads to elevated oxidative
903   stress and acceleration of age-dependent skeletal muscle atrophy. *Free Radical
904   Biology and Medicine*, *40*(11), 1993–2004.
905 Nowicka, M., & Robinson, M. D. (2016). DRIMSeq: a Dirichlet-multinomial framework
906   for multivariate count outcomes in genomics. *F1000Research*, *5*.
907 Oka, S., Hirai, J., Yasukawa, T., Nakahara, Y., & Inoue, Y. H. (2015). A correlation of

908   reactive oxygen species accumulation by depletion of superoxide dismutases
909   with age-dependent impairment in the nervous system and muscles of
910   Drosophila adults. *Biogerontology*, *16*(4), 485–501.
911 Orr, W. C., Mockett, R. J., Benes, J. J., & Sohal, R. S. (2003). Effects of
912   Overexpression of Copper-Zinc and Manganese Superoxide Dismutases,
913   Catalase, and Thioredoxin Reductase Genes on Longevity in *Drosophila*
914   *melanogaster*. *Journal of Biological Chemistry*, *278*(29), 26418–26422.
915   doi:10.1074/jbc.M303095200
916 Orsini, L., Brown, J. B., Shams Solari, O., Li, D., He, S., Podicheti, R., … others.
917   (2018). Early transcriptional response pathways in *Daphnia magna* are
918   coordinated in networks of crustacean-specific genes. *Molecular Ecology*, *27*(4),
919   886–897.
920 Orsini, L., Gilbert, D., Podicheti, R., Jansen, M., Brown, J. B., Solari, O. S., …
921   Frilander, M. J. (2016). *Daphnia magna* transcriptome by RNA-Seq across 12
922   environmental stressors. *Scientific Data*, *3*, 160030.
923 Patro, R., Duggal, G., Love, M. I., Irizarry, R. A., & Kingsford, C. (2017). Salmon
924   provides fast and bias-aware quantification of transcript expression. *Nature*
925   *Methods*, *14*(4), 417–419. doi:10.1038/nmeth.4197
926 Pinzón, N., Li, B., Martinez, L., Sergeeva, A., Presumey, J., Apparailly, F., & Seitz,
927   H. (2017). microRNA target prediction programs predict many false positives.
928   *Genome Research*, *27*(2), 234–245.
929 Quinlan, A. R., & Hall, I. M. (2010). BEDTools: a flexible suite of utilities for
930   comparing genomic features. *Bioinformatics*, *26*(6), 841–842.
931   doi:10.1093/bioinformatics/btq033
932 Redman, L. M., & Ravussin, E. (2011). Caloric restriction in humans: impact on
933   physiological, psychological, and behavioral outcomes. *Antioxidants & Redox*
934   *Signaling*, *14*(2), 275–287.
935 Regan, J. C., Khericha, M., Dobson, A. J., Bolukbasi, E., Rattanavirotkul, N., &
936   Partridge, L. (2016). Sex difference in pathology of the ageing gut mediates the
937   greater response of female lifespan to dietary restriction. *Elife*, *5*, e10956.
938 Rider, C. V, Gorr, T. A., Olmstead, A. W., Wasilak, B. A., & LeBlanc, G. A. (2005).
939   Stress signaling: coregulation of hemoglobin and male sex determination
940   through a terpenoid signaling pathway in a crustacean. *Journal of Experimental*
941   *Biology*, *208*(1), 15 LP – 23. doi:10.1242/jeb.01343
942 Rubio-Patiño, C., Bossowski, J. P., De Donatis, G. M., Mondragón, L., Villa, E., Aira,
943   L. E., … others. (2018). Low-protein diet induces IRE1α-dependent anticancer
944   immunosurveillance. *Cell Metabolism*, *27*(4), 828–842.
945 Russell, S. J., & Kahn, C. R. (2007). Endocrine regulation of ageing. *Nature Reviews*
946   *Molecular Cell Biology*, *8*(9), 681.
947 Sanchez, D., López-Arias, B., Torroja, L., Canal, I., Wang, X., Bastiani, M. J., &
948   Ganfornina, M. D. (2006). Loss of glial lazarillo, a homolog of apolipoprotein D,
949   reduces lifespan and stress resistance in *Drosophila*. *Current Biology*, *16*(7),
950   680–686.
951 Seidl, M. D., Paul, R. J., & Pirow, R. (2005). Effects of hypoxia acclimation on
952   morpho-physiological traits over three generations of *Daphnia magna*. *Journal of*
953   *Experimental Biology*, *208*(11), 2165–2175.
954 Sohal, R. S., & Weindruch, R. (1996). Oxidative Stress, Caloric Restriction, and
955   Aging. *Science*, *273*(5271), 59–63.
956 Soneson, C., Love, M. I., & Robinson, M. D. (2015). Differential analyses for RNA-
957   seq: transcript-level estimates improve gene-level inferences. *F1000Research*,

958 *4.*

959 Steinkraus, K. A., Smith, E. D., Davis, C., Carr, D., Pendergrass, W. R., Sutphin, G.
960   L., … Kaeberlein, M. (2008). Dietary restriction suppresses proteotoxicity and
961   enhances longevity by an hsf-1-dependent mechanism in *Caenorhabditis*
962   *elegans. Aging Cell, 7*(3), 394–404.

963 Stephens, M. (2016). False discovery rates: a new deal. *Biostatistics, 18*(2), 275–
964   294.

965 Supek, F., Bošnjak, M., Škunca, N., & Šmuc, T. (2011). REVIGO summarizes and
966   visualizes long lists of gene ontology terms. *PloS One, 6*(7), e21800.

967 Tasaki, E., Kobayashi, K., Matsuura, K., & Iuchi, Y. (2018). Long-lived termite
968   queens exhibit high Cu/Zn-superoxide dismutase activity. *Oxidative Medicine*
969   *and Cellular Longevity, 2018.*

970 Thadani, R., & Tammi, M. T. (2006). MicroTar: predicting microRNA targets from
971   RNA duplexes. In *BMC bioinformatics* (Vol. 7, p. S20).

972 Vigne, P., & Frelin, C. (2006). A low protein diet increases the hypoxic tolerance in
973   Drosophila. *PLoS One, 1*(1).

974 Walford, R. L., Harris, S. B., & Weindruch, R. (1987). Dietary restriction and aging:
975   historical phases, mechanisms and current directions. *The Journal of Nutrition,*
976   *117*(10), 1650–1654.

977 Walker, D. W., Muffat, J., Rundel, C., & Benzer, S. (2006). Overexpression of a
978   *Drosophila* homolog of apolipoprotein D leads to increased stress resistance
979   and extended lifespan. *Current Biology, 16*(7), 674–679.

980 Wang, Y., Branicky, R., Noë, A., & Hekimi, S. (2018). Superoxide dismutases: Dual
981   roles in controlling ROS damage and regulating ROS signaling. *The Journal of*
982   *Cell Biology, 217*(6), 1915 LP – 1928. doi:10.1083/jcb.201708007

983 Wood, S. H., Dam, S., Craig, T., Tacutu, R., O'Toole, A., Merry, B. J., & de
984   Magalhães, J. P. (2015). Transcriptome analysis in calorie-restricted rats
985   implicates epigenetic and post-translational mechanisms in neuroprotection and
986   aging. *Genome Biology, 16*(1), 285.

987 Yu, G., Wang, L.-G., Han, Y., & He, Q.-Y. (2012). clusterProfiler: an R package for
988   comparing biological themes among gene clusters. *Omics: A Journal of*
989   *Integrative Biology, 16*(5), 284–287.

990 Zeis, B. (2020). Hemoglobin in Arthropods-*Daphnia* as a Model. In U. Hoeger & J. R.
991   Harris (Eds.), *Vertebrate and Invertebrate Respiratory Proteins, Lipoproteins*
992   *and other Body Fluid Proteins* (pp. 163–194). Cham: Springer International
993   Publishing. doi:10.1007/978-3-030-41769-7_6

994 Zeis, B., Becher, B., Goldmann, T., Clark, R., Vollmer, E., Bölke, B., … others.
995   (2003). Differential haemoglobin gene expression in the crustacean *Daphnia*
996   *magna* exposed to different oxygen partial pressures. *Biological Chemistry,*
997   *384*(8), 1133–1145.

998 Zhang, C., Zhang, B., Lin, L.-L., & Zhao, S. (2017). Evaluation and comparison of
999   computational tools for RNA-seq isoform quantification. *BMC Genomics, 18*(1),
1000   583.

1001 Zhang, Y., Shao, Z., Zhai, Z., Shen, C., & Powell-Coffman, J. A. (2009). The HIF-1
1002   hypoxia-inducible factor modulates lifespan in *C. elegans. PloS One, 4*(7).

1003 Zhu, A., Ibrahim, J. G., & Love, M. I. (2019). Heavy-tailed prior distributions for
1004   sequence count data: removing the noise and preserving large differences.
1005   *Bioinformatics, 35*(12), 2084–2092.

1006

1007

1008
1009
1010
1011
1012
1013
1014
1015
1016 **Data Accessibility**
1017

1018 Raw read data generated for this study has been deposited in the European

1019 Nucleotide Archive, Bioproject PRJEB25137.

1020
1021
1022 **Author Contributions**
1023
1024
1025 JH and TJL designed this research and wrote the paper. JH, TJL, PJW and JC

1026 performed research. PJW and JC maintained *D. magna* genotypes used in this

1027 study.

1028
1029 **Tables**
1030

1031 **Table 1. Significantly differentially expressed genes at each log$_2$-fold change**
1032 **threshold.** More genes were up-regulated in CR replicates.

	Log$_2$-fold change 0	Log$_2$-fold change >1	Log$_2$-old change >2
Up-regulated in CR	3345	280	62
Down-regulated in CR	3063	52	11

1033
1034
1035 **Table 2. Overlap between significantly expressed genes at log$_2$-fold change 0**
1036 **and hypo- or hyper-methylated genes.** Percentages were calculated from total
1037 hypo- and hyper-methylated genes.

	Up-regulated in CR	Down-regulated in CR
Hypo-methylated	20 (10%)	48 (25%)
Hyper-methylated	16 (14%)	28 (24%)

1038

Table 3. Overlap between significantly expressed genes at log$_2$-fold change 0 (and log$_2$-fold change 2) and predicted correlation in expression between miRNA-mRNA pairs. A positive correlation means miRNA-mRNA pairs were both highly or lowly expressed, and a negative correlation that they exhibit reciprocal expression. Annotations for the genes in each category are given in Supplementary Table S9.

	Up-regulated in CR	Down-regulated in CR
Pearson's r > 0.5	33 (6)	5 (1)
Pearson's r < -0.5	33 (7)	4 (0)

Figures

Figure 1. CR *Daphnia magna* lived approximately 15 days longer than NF *D. magna* on average. A) Point estimates are mean longevity across clones for each treatment and whiskers are standard errors. B) Survivorship between treatments varied among the eight different *D. magna* genotypes (dashed line = NF, solid line = CR); Clone 32 is labelled in bold in the upper-left plot.

Figure 2. DESeq2 generated PCA plots of regularized logarithm transformation of data of replicates in the nutrition experiment. Shapes define treatment, and colour defines mother. Figure legend: NF = normal food, CR = caloric restriction. Dashed lines indicate relationship between replicates paired by mother; these are always divided along the x-axis in the same direction.

Figure 3. Transcript proportion plots and protein domains for differentially used transcripts of an up-regulated di-domain haemoglobin. Transcripts 11, 12, and 21 respectively of gene Dapma7bEVm014981 show DTU across conditions in DEXSeq and transcript 12 in DRIMSeq adjusted results. Bars represent proportions of total gene expression for that transcript per replicate and diamonds DRIMSeq fitted values: NF = normal food and CR = caloric restriction. Di-domain haemoglobin and erythrocruorin domains for transcript 12 are shown; arrows below indicate one erythrocruorin domain is missing in transcript 11 and none occur in transcript 21, although both still encode a di-domain haemoglobin like transcript 12.

Figure 4. REVIGO scatter plots of enriched biological process GO terms for Caloric Restriction *versus* Normal Food. GO terms are grouped by REVIGO into broader categories indicated by colour and legend, Circle size is –log$_{10}$ of the topGO enrichment p-value with scales inset next to each plot. A) Higher expression in CR Biological Process GO terms, B) Higher expression in NF Biological Process GO terms C) Higher expression in CR molecular function GO terms C) Higher expression in CR molecular function GO terms, D) Higher expression in NF molecular function GO terms. GO terms associated with numbers can be found in Supplementray Table S10.

Figure 5. Gene Set Enrichment Analysis ridge plot for significant KEGG terms. Ridge plots are density plots of the frequency of log$_2$ fold-change values per gene within each enriched KEGG group, which helps to interpret the up- or down-regulation of that KEGG category. The plot was created in clusterProfiler using

1081 KEGG orthologue annotations and log$_2$-fold changes per gene calculated by
1082 DESeq2 during differential expression analysis. X-axis is log$_2$-fold change in
1083 expression for genes present in each KEGG category plotted, with positive values
1084 indicating increased expression in CR replicates and negative values in NF
1085 replicates. Peaks are coloured by corrected p-value as shown by the legend and
1086 corrected p-value and q-values are shown per KEGG category. KEGG term
1087 definitions: K08852=serine/threonine-protein kinase/endoribonuclease IRE1;
1088 K03070=preprotein translocase subunit secA; K11715=serine/threonine-protein
1089 kinase/endoribonuclease IRE2; K01183=chitinase; K15001=cytochrome P450 family
1090 4; K03098=apolipoprotein D and lipocalin family protein.

1091 **Supplementary Tables**

1092

1093 **Supplementary Table S1.** Raw and filtered reads per replicate included in this
1094 experiment.

1095

1096 **Supplementary Table S2.** DESeq2 output for significant genes at log$_2$-fold change
1097 0. Column 1 = gene name, column 2 = mean expression level of gene, column 3 =
1098 log in base two fold change, column 4 = log$_2$-fold change standard error, column 5 =
1099 p-value, column 6 = false discovery rate adjusted p-value.

1100

1101 **Supplementary Table S3.** DESeq2 output for significant genes at log$_2$-fold change
1102 1. Column 1 = gene name, column 2 = mean expression level of gene, column 3 =
1103 log in base two fold change, column 4 = log$_2$-fold change standard error, column 5 =
1104 s-value.

1105

1106 **Supplementary Table S4.** DESeq2 output for significant genes at log$_2$-fold change
1107 2. Column 1 = gene name, column 2 = mean expression level of gene, column 3 =
1108 log in base two fold change, column 4 = log$_2$-fold change standard error, column 5 =
1109 s-value.

1110

1111 **Supplementary Table S5.** Gene annotations and expression levels in TPM for
1112 significant genes with higher expression under caloric restriction and higher under
1113 normal food respectively: 1 and 2 = genes expressed at greater than 10000 mean for
1114 log$_2$-fold change 0; 3 and 4 = all expression levels for log$_2$-fold change 1; 5 and 6 =
1115 all expression levels for log$_2$-fold change 2.

1116

1117 **Supplementary Table S6.** Molecular function GO terms enriched in differentially
1118 expressed genes at each log$_2$-fold change level after enrichment testing in topGO at
1119 alpha = 0.05. GO.ID = GO term identifier, Term = description of GO term, Annotated
1120 = number of genes annotated with this term, Significant = number of significant
1121 genes for the specified contrast annotated with this term, Expected = expected
1122 number of significant genes for the specified contrast annotated with this term,
1123 weight01 = p-value for GO term.

1124

1125 **Supplementary Table S7.** Biological Process GO terms enriched in differentially
1126 expressed genes at each log$_2$-fold change level after enrichment testing in topGO at
1127 alpha = 0.05. GO.ID = GO term identifier, Term = description of GO term, Annotated
1128 = number of genes annotated with this term, Significant = number of significant
1129 genes for the specified contrast annotated with this term, Expected = expected

1130   number of significant genes for the specified contrast annotated with this term,
1131   weight01 = p-value for GO term.

1132

1133   **Supplementary Table S8.** mRNA-miRNA pairs predicted by at least four of five
1134   tools.   mrna   =   *Daphnia*   gene,   mirna   =   *Daphnia*   miRNA,
1135   microtar/miranda/pita/rna22/rnahybrid = target prediction tool, binding_sites =
1136   number of binding sites in 3' UTRs of mRNA, no_tools = number of tools that
1137   predicted a binding site, closest miRbase homolog = as identified in supplementary
1138   table S4 of Hearn et al (2018).

1139

1140   **Supplementary Table S9.** Gene descriptions for genes included in Table 3,
1141   annotations for genes in each of the four possible combinations are given. CR =
1142   caloric restriction.

1143

1144   **Supplementary Table S10.** GO terms for each numbered circle in Figure 4.

1145

1146   **Supplementary Files**

1147

1148   **Supplementary File S1**. R code used to analyse clone survival at each food level
1149   and model outputs in part 1, R code to identify differential gene expression using
1150   DESeq2 in part 2, and differential transcript usage using DEXSeq, DRIMSeq and
1151   stageR in part 3, topGo functional enrichment in part 4, and clusterProfiler gene set
1152   enrichment analysis in part 5, R code for creating REVIGO-derived scatter plots of
1153   enriched GO terms in part 6.

1154

1155   **Supplementary File S2.** Raw clone longevity data for all eight clones input into R
1156   survival analysis; R code given in Supplementary File S1, part 1.

1157

1158   **Supplementary File S3.** MultiQC results for FastQC read data-quality assessment,
1159   this file is in html format.

1160

1161   **Supplementary File S4**. DRIMSeq proportion plots for the 112 genes with
1162   significant differential transcript usage in common between DESeq and DRIMSeq.
1163   There are two plots per gene, one a barplot and the other a line plot.

1164   **Supplementary File S5. Correlation of methylation proportion and mean**
1165   **expression for caloric restriction and normal food datasets.** Methylation data
1166   adapted from (Hearn, Pearson, et al., 2019). For CR and NF 2029 and 2033 genes
1167   respectively with a methylation rate greater than 5%, a TPM expression mean over
1168   10 and non-overlapping genome annotation were included, and the Y-axis was
1169   limited to a TPM expression of 10000. Kendall's tau and Spearman's rho values are
1170   inset, Bonferroni-Holm corrected p-values for all correlations were highly significant
1171   at $p < 1 \times 10^{-6}$. The regression line in blue with grey confidence intervals is for
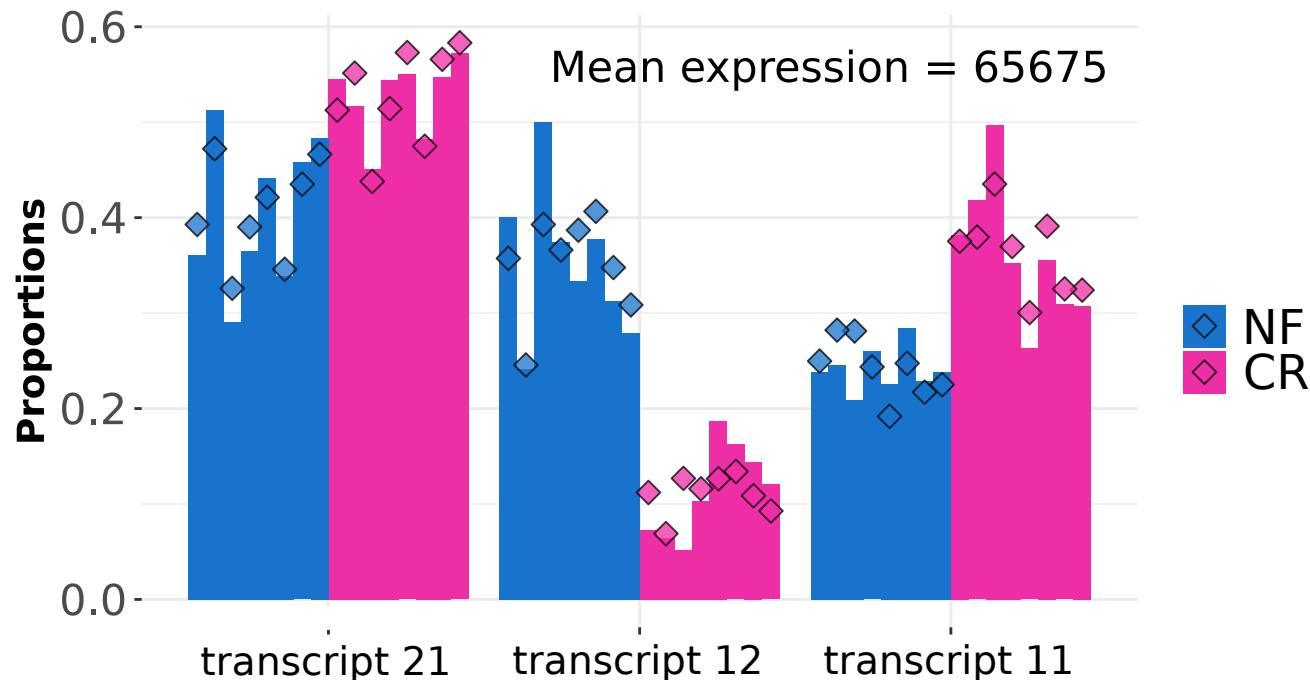1172   Kendall's tau correlations.

1173

1174

Mean expression = 65675
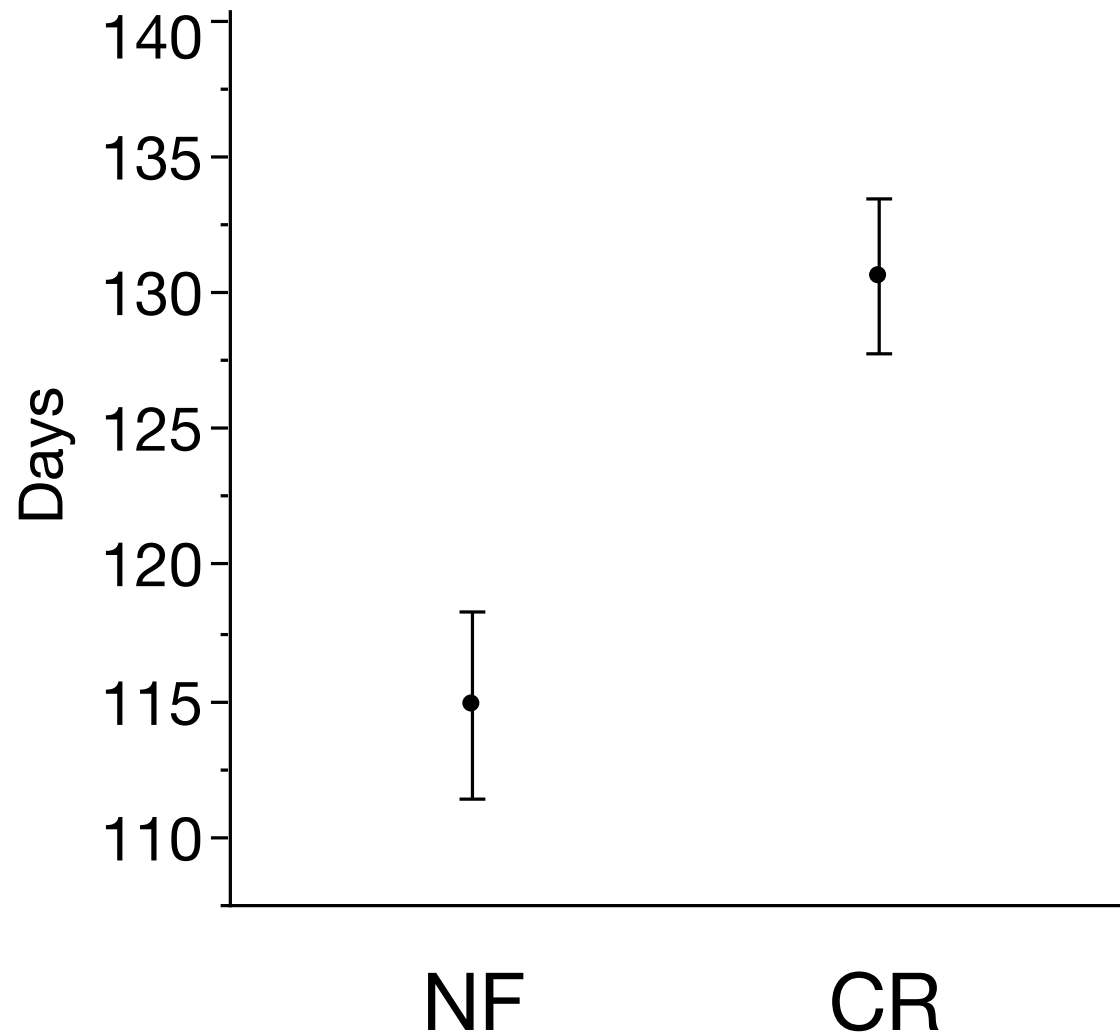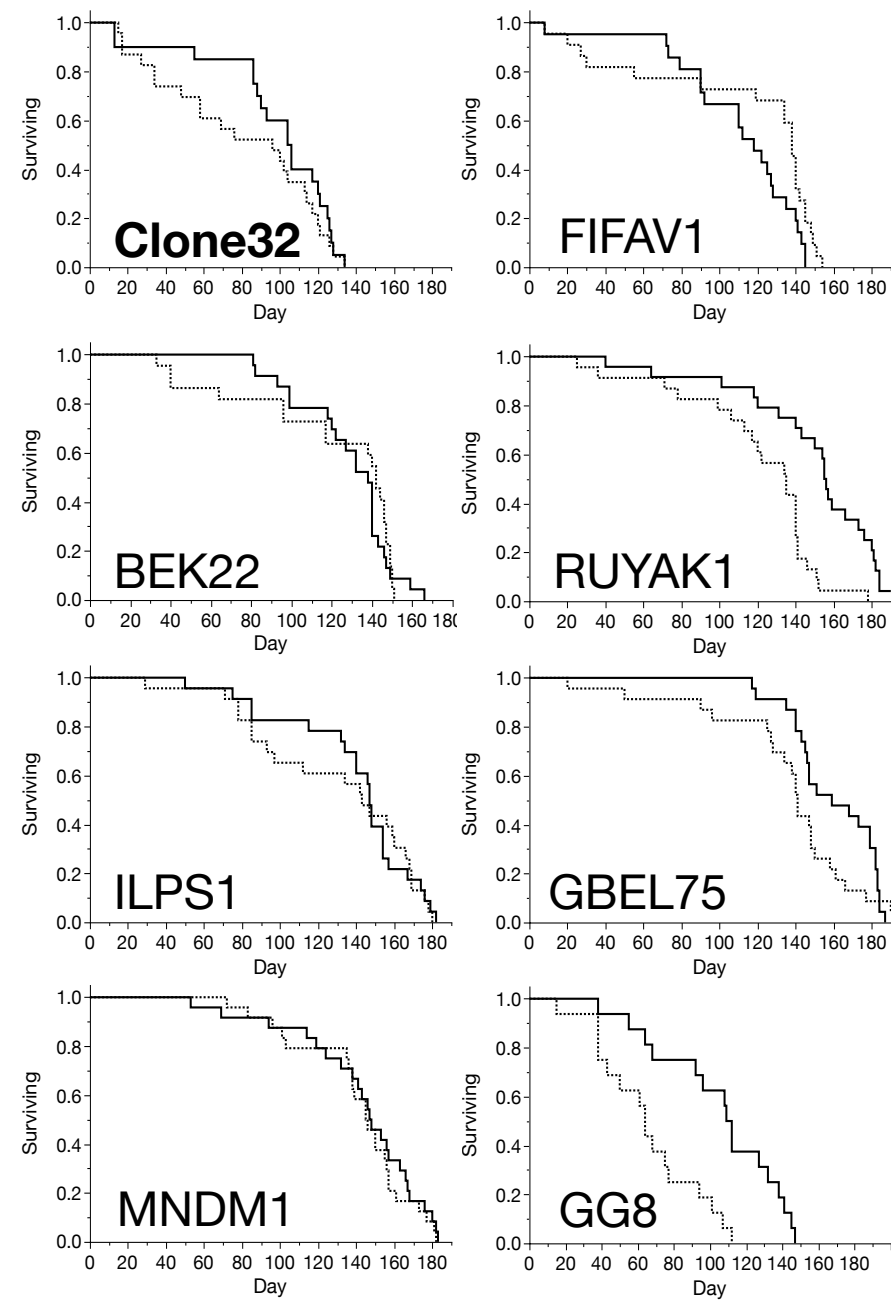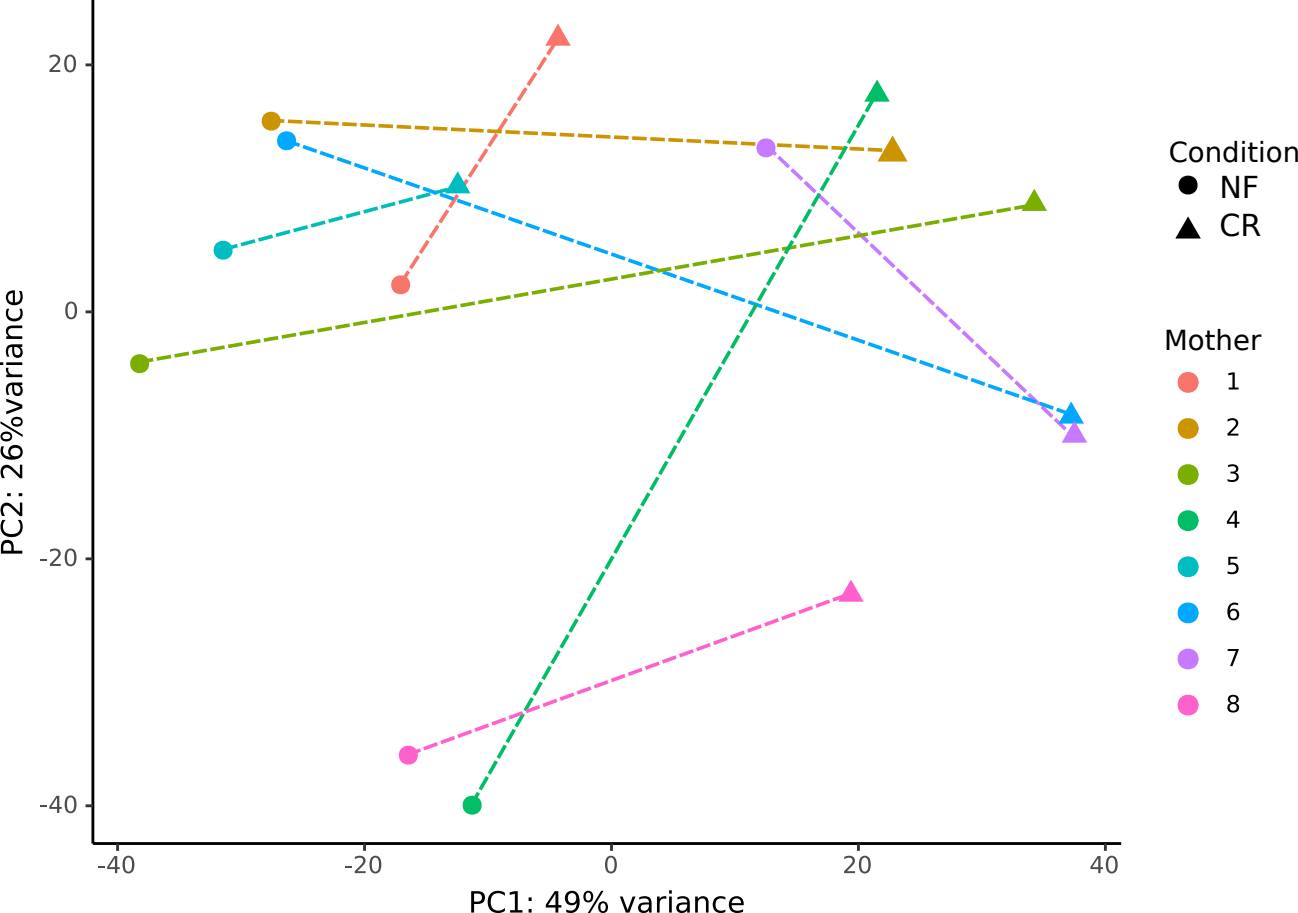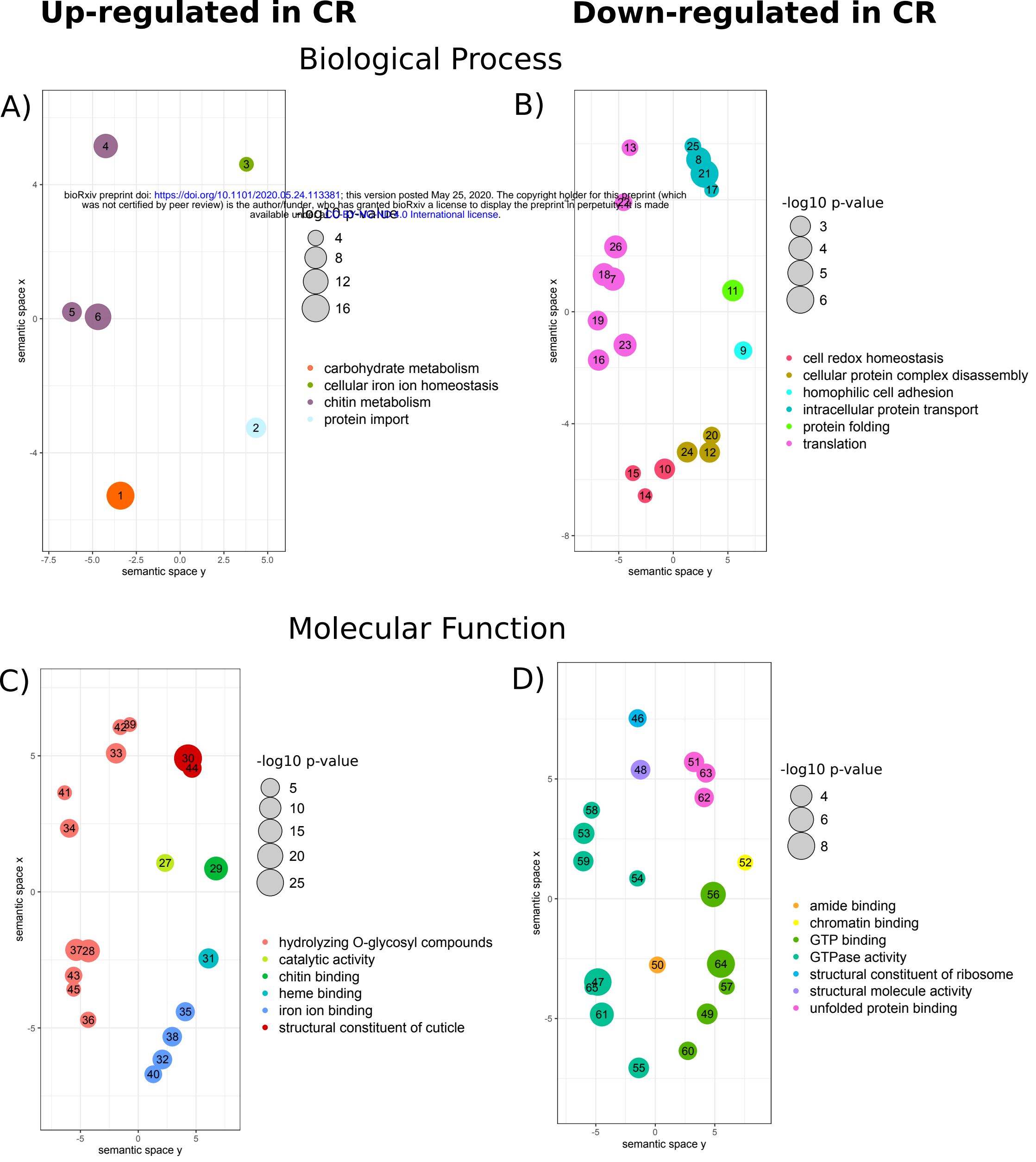
Dapma7bEVm014981 transcript 12 Di-domain Haemoglobin

Globin/Protoglobin

Globin-like superfamily

Erythrocruorin domains

Erythrocruorin domains not present in transcript 21

Erythrocruorin domain not present in transcript 11

Up-regulated in CR

Down-regulated in CR

Biological Process

Molecular Function